Bearing Capacity of Strip Footing Placed on Reinforced Cohesionless Soil Slope Using Conic Programming

Koushik Halder and Debarghya Chakraborty

Abstract By using lower bound finite element limit analysis technique with the combination of conic programming, the present study computes the bearing capacity of strip footing placed on the edge of a reinforced cohesionless soil slope and also subjected to a surcharge load. The bearing capacity factors (i) N_q associated with overburden pressure and (ii) N_γ associated with soil unit weight are computed by varying footing setback distance (b), soil friction angle (ϕ), and placement depth of reinforcement layer (d). The bearing capacity factors of the strip footing placed on the reinforced slope are found to be higher than that obtained for a strip footing situated on the unreinforced slope. The efficacy of the reinforcement layer is expressed in terms of dimensionless factors, η_q and η_γ which are the ratio of N_q and N_γ values obtained for the reinforced slope to the unreinforced slope. However, the maximum effectiveness of the reinforcement layer ($\eta_{q\text{-max}}$ and $\eta_{\gamma\text{-max}}$) is achieved when it is placed at an optimum distance (d_{cr}) from the footing base. The magnitude of the efficiency factors increases if the reinforcement layer is embedded in a soil having higher soil friction angle and it is also found that the increment is more in case of $\eta_{\gamma\text{-max}}$. In contrast, the effectiveness of reinforcement is found to be maximum when footing is placed at the slope edge. The use of conic programming is found to be effective as the computational time reduces in comparison to linear programming during the computation of N_q and N_γ.

Keywords Strip footing · Reinforced slope · Lower bound limit analysis · Conic programming

K. Halder (✉) · D. Chakraborty
Indian Institute of Technology Kharagpur, Kharagpur 721302, India
e-mail: koushikhalder@iitkgp.ac.in

D. Chakraborty
e-mail: debarghya@civil.iitkgp.ac.in

A. K. Dey et al. (eds.), *Proceedings of the 7th Indian Young Geotechnical Engineers Conference*, Lecture Notes in Civil Engineering 195,
https://doi.org/10.1007/978-981-16-6456-4_6

1 Introduction

Safe design of foundations for various structures such as buildings, bridge abutments, electrical transmission towers etc. situated on foothills and sloping grounds is a challenging task. The reduction in the load-bearing capacity and increasing chances of slope instability make these structures more vulnerable than the structures situated on the level ground [1–3]. With the advancement of reinforced earth technology, a number of laboratory-based model tests [4–6] as well as numerical studies [5, 7–10] were carried out to investigate the effect of reinforcement on the performance of both footing and slope. The laboratory-based experimental studies have shortcomings regarding the generalization point of view; they were very much case specific. On the other hand, Latha and Rajagopal [7] used finite element method; Alamshahi and Hataf [5] used finite element software Plaxis; Halder and Chakraborty [8, 9] used lower bound limit analysis method with linear programming. It is to be mentioned that the lower bound limit analysis technique is found to be advantageous than other methods on the following points: (1) the shape of the failure surface is not required to be presumed before the analysis, (ii) only shear strength parameters of soil (cohesion and friction angle) are required to be considered. The authors [8, 9] have used linear programming in their earlier works where failure surface was linearized by a polygon according to the formulation of Boterro et al. [11]. However, the linearization of yield surface generates a large number of inequality constraints which in turn increase the computational time. A non-linear programming technique can overcome the deficiencies raised by the implementation of linear programming. Among the available non-linear programming techniques, the second-order cone programming (SOCP), formulated by Makrodimopoulos and Martin [12] is advantageous as in case of SOCP formulation, the yield function is not required to be non-differentiable at some points, and thus there is no need of smoothening of yield surface either on the corners of the hexagon or at its apex [13]. Various researchers [13–15] used SOCP with lower bound limit analysis in solving various geotechnical problems in recent years. In addition to that according to the authors knowledge, no research studies were conducted till now for the computation of the bearing capacity factor (N_q) of a strip footing placed on the reinforced soil slope and subjected to surcharge loading.

Therefore, the present study computes the bearing capacity factors (N_q and N_γ) of a strip footing placed on the top of the reinforced cohesionless soil slope by using the lower bound finite element limit analysis technique with the non-linear programming. Reinforcement is modeled as per the formulation of Chakraborty and Kumar [16]. The influence of soil friction angle (ϕ), footing setback distance (b), and placement depth of reinforcement layer (d) on the computed values of N_q and N_γ are studied.

2 Problem Domain and Mesh Details

The two-dimensional plane strain problem domain used in the present study is illustrated by Fig. 1. The surface strip footing of width B is situated at a distance of b from the slope edge. The footing is subjected to a non-inclined and non-eccentric compressive load Q_u. A uniform surcharge of q is also acted over the horizontal line AB of the problem domain. The slope is inclined at an angle of 25°. A single layer of reinforcement is laid at a distance of d from the footing base. The frictional soil fill of the slope is assumed to follow Mohr–Coulomb constitutive model and associative flow rule. Similar to Chakraborty and Kumar [16], the effect of reinforcement in the analysis is considered by modifying stress discontinuities along the reinforcement-soil interface layer. Figure 1 shows that the domain is extended up to 12.80B in the horizontal direction and from 12.04B in the downward direction. While choosing the size of the problem domain it is ensured that (i) failure stresses should not reach to the domain boundary, and (ii) magnitude of collapse load should not change abruptly with the change in the size of the problem domain. The normal and shear stresses applied along the horizontal ground surface (GH and IJ) and slope face (JK) are equal to q and zero, respectively. Roughness between footing and soil interface along HI line is implemented with the help of equation $|\tau_{xy}| \leq (c - \sigma_y \tan\varphi)$.

Three noded triangular elements are used to discretize the problem domain. A relatively denser mesh is chosen near the singularity point below the two corners of the footing edge while a coarser mesh is created near the boundary region. According to the plane strain formulation of Sloan [17], each node consists of three unknown stresses; (i) two normal stresses in x (σ_x) and y (σ_y) direction, and (ii) shear stress

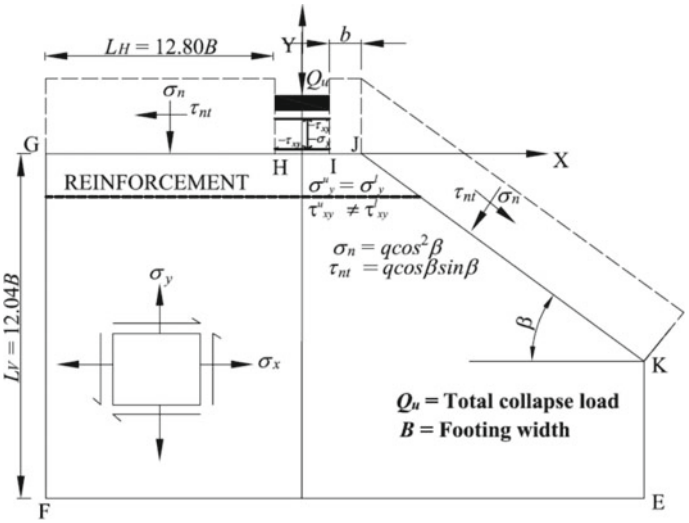

Fig. 1 Problem domain

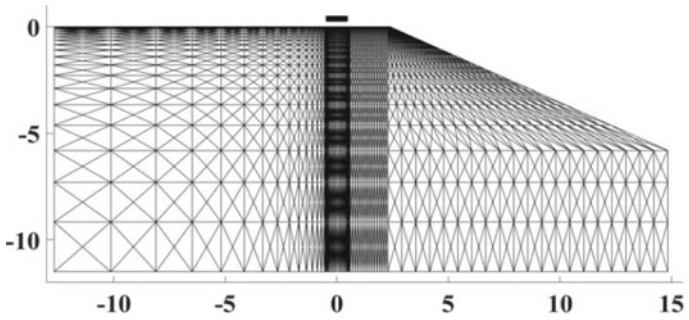

Fig. 2 FE mesh used in the analysis

(τ_{xy}). A typical mesh discretization of the slope having $\beta = 25°$, $\phi = 30°$, and $b/B = 2$ is shown in Fig. 2 where N, E, D_c, and N_i represent the total number of (i) nodes, (ii) elements, (iii) discontinuities, and (iv) nodes along footing-soil interface, respectively.

3 Methodology

The lower bound value of the collapse load of footing is obtained in the present study by employing the plane strain lower bound formulation of Sloan [17]. According to Sloan [17], the admissible stress field would furnish the lower bound solution after the satisfaction of (i) element equilibrium condition throughout the problem domain, (ii) stress boundary conditions at the boundary edges, (iii) stress discontinuity conditions along the line of stress discontinuity formed by two adjacent triangles, and (iv) yield criterion at all the nodes of the elements. No external element is used to model the reinforcement layer. The reinforcement modeling is done by following the formulation of Chakraborty and Kumar [16]. Chakraborty and Kumar [16] modified the stress discontinuities along the reinforcement-soil interface layer. Shear stresses were set aside discontinuous along the reinforcement-soil interface layer, but normal stresses were permitted. Whereas, in all other places, both the normal and shear stresses were kept continuous along the edges of discontinuity. Due to the implementation of element equilibrium, stress boundary, and stress discontinuity conditions, equality constraints are generated. As mentioned earlier, a non-linear programming technique, SOCP is used in the present study instead of linear programming as suggested by Sloan [17]. According to the SOCP formulation, the Mohr–Coulomb yield surface is used in the form of a conic quadratic constraints with the use of auxiliary variables. A set of inequality constraints are thus generated. After the generation of equality and inequality constraints, the objective function (collapse load) is then maximized. The expression of the objective function is obtained with the numerical integration of normal stresses along the nodes representing footing. One can follow the work of

Sloan [17] for the detailed formulation of lower bound finite element limit analysis and the work of Tang et al. [13] for the SOCP formulation. Here, only the final form of the optimization scheme is presented in Eqs. 1 and 2.

Maximize

$$\{g\}^T\{\sigma\} \tag{1}$$

subjected to

$$[A]\{\sigma\} = \{B\} \tag{2}$$

whereas,

$$\begin{bmatrix} A_{\mathrm{EQ}} & 0 \\ A_{\mathrm{SB}} & 0 \\ A_{\mathrm{DS}} & 0 \\ A_{\mathrm{SC}} & I \end{bmatrix} \quad \{b\} = \begin{Bmatrix} b_{\mathrm{EQ}} \\ b_{\mathrm{SB}} \\ b_{\mathrm{DS}} \\ b_{\mathrm{SC}} \end{Bmatrix} \tag{3}$$

In the above expressions, $\{g^T\}$ is the vector consists of the coefficients obtained from the objective function; $\{\sigma\}$ is the global stress vector; $[A_{\mathrm{EQ}}]$, $[A_{\mathrm{SB}}]$, and $[A_{DS}]$ are the matrices comprised of right-hand side coefficients from constraints obtained after the employment of equilibrium, stress boundary, and stress discontinuity conditions. $[I]$ is the identity matrix. Whereas, $\{b_{\mathrm{EQ}}\}$, $\{b_{\mathrm{SB}}\}$, and $\{b_{\mathrm{DS}}\}$ are the vectors composed of left-hand side coefficients of the constraints generated due to the fulfillment of equilibrium, stress boundary, and stress discontinuity conditions. A code is written in MATLAB [18] to carry out the lower bound limit analysis. An optimization toolbox MOSEK [19] is used for carrying out non-linear programming.

4 Results

Figure 3 shows the variation between the efficiency factors (η_{q} and η_{γ}) and placement depth of reinforcement for various combinations of ϕ and b/B. Two values of friction angle ($\phi = 30°$ and 40°) of the cohesionless soil fill are considered. The strip footing is placed at three setback distances (b/B) of 0, 2, and 4. The magnitudes of the efficiency factors (η_{q} and η_{γ}) increase rapidly after a certain value of d/B, after that it reduces drastically. The placement depth of reinforcement where efficiency factors attain the maximum value ($\eta_{\mathrm{q\text{-}max}}$ or $\eta_{\gamma\text{-}\mathrm{max}}$) is known as optimum depth of placement of the reinforcement (d_{cr}/B). The magnitude of the $\eta_{\mathrm{q\text{-}max}}$ and $\eta_{\gamma\text{-}\mathrm{max}}$ increases if the reinforcement layer is embedded in a soil having higher soil friction angle. As an example for a slope having $\beta = 25°$, $b/B = 0$, the magnitude of $\eta_{\mathrm{q\text{-}max}}$ increases from 1.56 to 1.71 and the value of $\eta_{\gamma\text{-}\mathrm{max}}$ enhances from 1.68 to 1.79 with the change in ϕ value from 30° to 40°. Figure 3 shows that the optimum depth of placement required

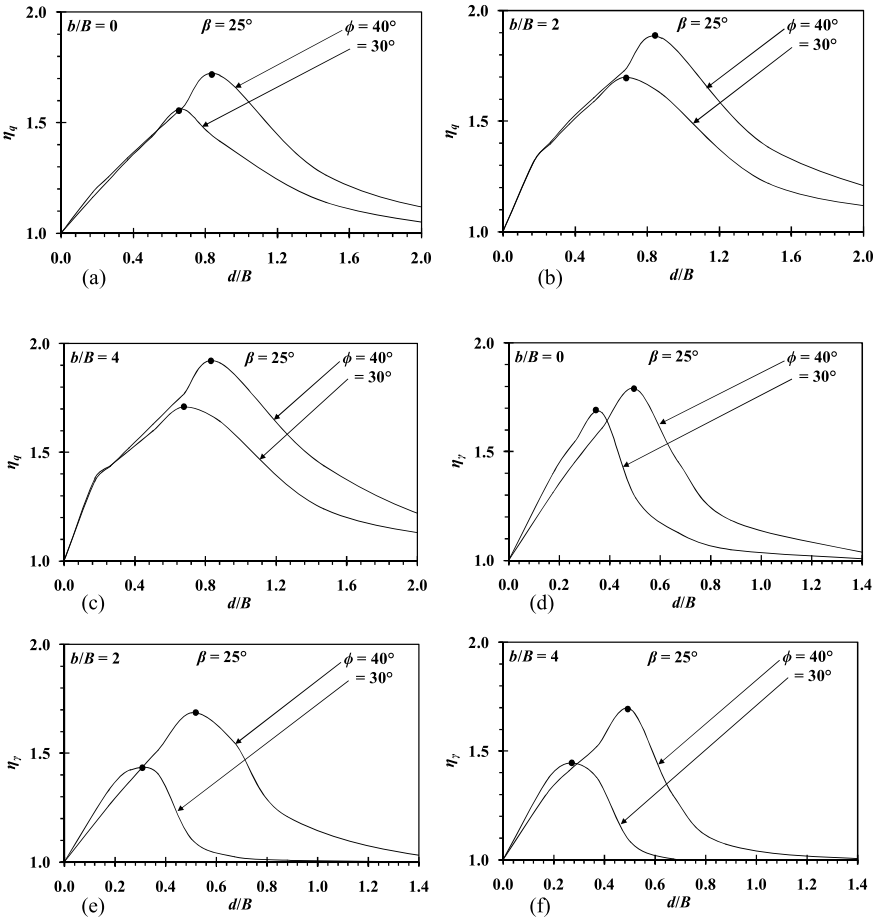

Fig. 3 Variation of η_q with d/B of a reinforced slope having $\beta = 25°$, $\phi = 30°$, 40° and **a** $b/B = 0$; **b** $b/B = 2$; **c** $b/B = 4$; variation of η_γ with d/B of a reinforced slope having $\beta = 25°$, $\phi = 30°$, 40° and **d** $b/B = 0$; **e** $b/B = 2$; **f** $b/B = 4$

to obtain the value of $\eta_{\gamma\text{-max}}$ is found to be higher than that required to obtain the value of $\eta_{q\text{-max}}$. The value of η_γ is found to be maximum when footing is placed on the edge of the slope rather than at a distance from the slope edge. As an instance for a slope having $\beta = 25°$ and $\phi = 30°$, the magnitude of $\eta_{\gamma\text{-max}}$ reduces from 1.68 to 1.42 with the increment in the value of b/B from 0 to 4.

Table 1 Comparison between the values of $\eta_{\gamma\text{-max}}$ and d_{cr}/B obtained from present study and Halder and Chakraborty [8]

$\beta = 25°, \phi = 30°$				
b/B	Present Study		Halder and Chakraborty [8]	
	$\eta_{\gamma\text{-max}}$	d_{cr}/B	$\eta_{\gamma\text{-max}}$	d_{cr}/B
0	1.68	0.37	1.70	0.31
2	1.44	0.26	1.49	0.31
4	1.42	0.26	1.46	0.31

4.1 Comparison

The magnitude of $\eta_{\gamma\text{-max}}$ and d_{cr}/B obtained from the present study is compared with the obtained results from Halder and Chakraborty [8] for a slope configuration of $\beta = 25°$, $\phi = 30°$, and $b/B = 0$, 2, and 4 (refer Table 1). Halder and Chakraborty [8] used lower bound finite element limit analysis technique with linear programming. It is found that in all of the cases present value matches well with the reported results of Halder and Chakraborty [8]. However, the present value is lower than the reported value.

5 Failure Patterns

Failure mechanisms of both unreinforced and reinforced slopes are shown in Figs. 3a–f after plotting the state of stresses of any point after failure in two-dimensional object space. In the Fig. 3, a/f equal to one denotes the state of shear failure. By contrast, for all those non-yielding points, the value of a/f is less than one. The value of a and f is obtained from following equations:

$$a = \left(\sigma_x - \sigma_y\right)^2 + \left(2\tau_{xy}\right)^2, \text{ and } f = \left[-\left(\sigma_x + \sigma_y\right)\sin\varphi\right]^2 \tag{4}$$

Figure 4a–c show failure mechanisms of both unreinforced and reinforced slopes when footing is positioned at the slope edge. For both unreinforced and reinforced slopes (refer Fig. 4a–b), failure zone in the LHS of the footing is visibly truncated and the failure zone in the RHS of the footing easily reaches to the slope face.

However, with the inclusion of a reinforcement layer, the plastic zone of the failure surface propagates more in the downward direction, which in turn increases the bearing capacity of the footing. Figure 4c shows that when reinforcement is placed at a deeper depth, failure surface propagates over the reinforcement layer. Figure 4d–f illustrate that when footing is placed at a setback distance of 4, plastic zone develops on both sides of the footing, irrespective of unreinforced or reinforced slope. It is quite similar to the failure patterns obtained for the footing placed on the level ground.

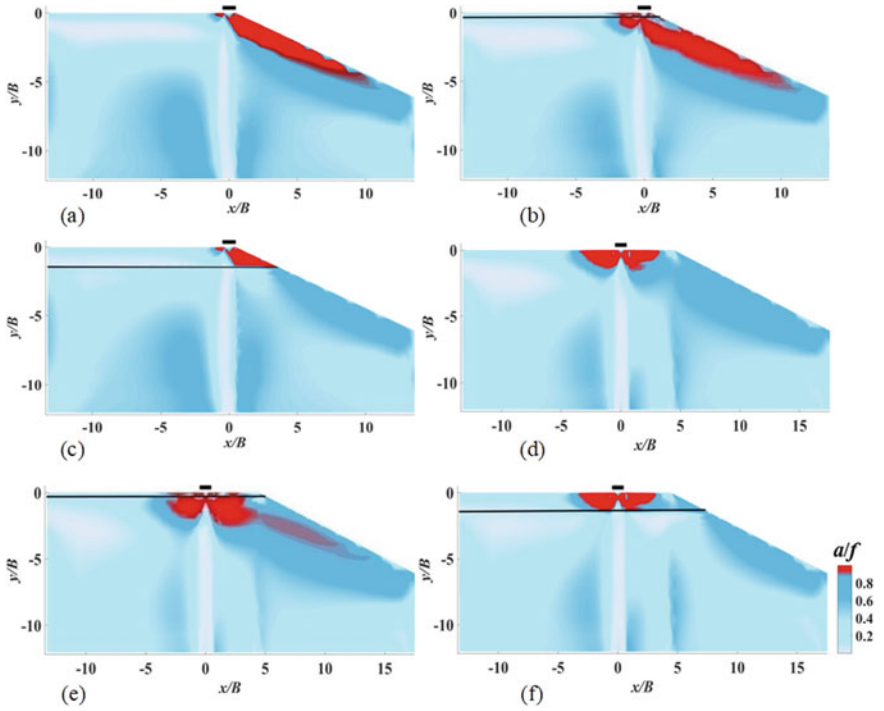

Fig. 4 Failure patterns obtained for a slope of $\beta = 25°$, $\phi = 30°$ with **a** unreinforced, $b/B = 0$; **b** reinforcement at optimum depth, $b/B = 0$; **c** reinforcement at higher depth, $b/B = 0$; **d** unreinforced, $b/B = 4$; **e** reinforcement at optimum depth, $b/B = 4$; **f** reinforcement at higher depth, $b/B = 4$

6 Conclusions

By using the lower bound finite element limit analysis technique with conic programming, the bearing capacity factors (N_q and N_γ) are obtained for a strip footing placed on the top of the reinforced cohesionless soil slopes. The inclusion of a single layer of reinforcement is found to be very effective as both the values of N_q and N_γ increase by a significant amount. This increment is observed to be highest when footing is placed on the slope edge. The magnitude of N_q and N_γ for strip footing situated on the edge of a reinforced slope of $\beta = 25°$ and $\phi = 30°$ increases by 1.56 and 1.68 times than that obtained for strip footing placed on the unreinforced slope.

References

1. Meyerhof GG (1963) Some recent research on the bearing capacity of foundations. Can Geotech J 1(1):16–26
2. Kumar J, Chakraborty D (2013) Seismic bearing capacity of foundations on cohesionless slopes. J Geotech Geoenviron Eng 139(11):1986–1993
3. Halder K, Chakraborty D, Dash SK (2019) Bearing capacity of a strip footing situated on soil slope using a non-associated flow rule in lower bound limit analysis. Int J Geotech Eng 13(2):103–111
4. Selvadurai A, Gnanendran C (1989) An experimental study of a footing located on a sloped fill: influence of a soil reinforcement layer. Can Geotech J 26(3):467–473
5. Alamshahi S, Hataf N (2009) Bearing capacity of strip footings on sand slopes reinforced with geogrid and grid-anchor. Geotext Geomembr 27(3):217–226
6. Mehrjardi GT, Ghanbari A, Mehdizadeh H (2016) Experimental study on the behaviour of geogrid-reinforced slopes with respect to aggregate size. Geotext Geomembr 44(6):862–871
7. Latha GM, Rajagopal K (2007) Parametric finite element analyses of geocell-supported embankments. Can Geotech J 44(8):917–927
8. Halder K, Chakraborty D (2018) Bearing capacity of strip footing placed on the reinforced soil slope. Int J Geomech 18(11):06018025
9. Halder K, Chakraborty D (2019) Effect of interface friction angle between soil and reinforcement on the bearing capacity of strip footing placed on the reinforced slope. Int J Geomech 19(5):06019008
10. Halder K, Chakraborty D (2018) Probabilistic stability analyses of reinforced slope subjected to strip loading. Geotech Eng J SEAGS AGSSEA 49(4):92–99
11. Bottero A, Negre R, Pastor J, Turgeman S (1980) Finite element method and limit analysis theory for soil mechanics problems. Comput Methods Appl Mech Eng 22(1):131–149
12. Makrodimopoulos A, Martin CM (2006) Lower bound limit analysis of cohesive-frictional materials using second-order cone programming. Int J Numer Meth Eng 66(4):604–634
13. Tang C, Phoon KK, Toh KC (2014) Lower-bound limit analysis of seismic passive earth pressure on rigid walls. Int J Geomech 14(5):04014022
14. Sahoo JP, Khuntia S (2018) Lower bound solutions for uplift capacity of strip anchors adjacent to sloping ground in clay. Mar Georesour Geotechnol 36(4):405–416
15. Kumar J, Rahaman O (2019) Vertical uplift resistance of horizontal plate anchors for eccentric and inclined loads. Can Geotech J 56(2):290–299
16. Chakraborty D, Kumar J (2014) Bearing capacity of strip foundations in reinforced soils. Int J Geomech 14(1):45–58
17. Sloan SW (1988) Lower bound limit analysis using finite elements and linear programming. Int J Numer Anal Meth Geomech 12(1):61–77
18. Matlab 8.5 [Computer software]. Natick, MA, MathWorks
19. MOSEK ApS version 8.0 [Computer software]. MOSEK, Copenhagen, Denmark